

ON THE TEMPERATURE–EMISSION MEASURE DISTRIBUTION IN STELLAR CORONAE

PETER J. CARGILL¹ AND JAMES A. KLIMCHUK²
Received 2005 October 13; accepted 2005 December 21

ABSTRACT

Strong peaks in the emission measure–temperature (EM– T) distributions in the coronae of some binary stars are associated with the presence of hot (10^7 K), dense (up to 10^{13} cm⁻³) plasma. These peaks are very reminiscent of those predicted to arise in an impulsively heated solar corona. A coronal model comprised of many impulsively heated strands is adapted to stellar parameters. It is shown that the properties of the EM– T distribution can be accounted for in general terms provided the emission comes from many very small loops (length under 10^3 km) with intense magnetic fields (1 kG) distributed across part of the surface of the star. The heating requires events that generally dissipate between 10^{26} and 10^{28} ergs, which is in the range of solar microflares. This implies that such stars must be capable of generating regions of localized intense magnetic fields.

Subject headings: binaries: general — stars: coronae

Online material: color figure

1. INTRODUCTION

The distribution of the emission measure as a function of temperature in the corona of the Sun and other stars provides important information about both the structure of the corona, and the process(es) responsible for its high temperature. The emission measure can be defined as $EM = \int n_e^2 dV$, where n_e is the electron density and V is the emitting volume. Under the assumption of ionization equilibrium, measurements of the intensity of a range of emission lines forming at known temperatures determine the EM– T relation. For the solar corona, $EM \propto T^{3/2}$ near 10^6 K, but information about the EM– T scaling above $2\text{--}3 \times 10^6$ K is minimal due to inadequate temperature coverage. If the emitting volume can be estimated, as is possible for the Sun, the assumption of a homogeneous plasma then permits a determination of the density. This will never be the real density, since sub-resolution filamentary structures will be present, with radiation coming from only a subset of the measured volume. However, the real density can be determined from suitable pairs of density-sensitive lines, and one can then determine the actual volume responsible for the radiation, and hence the scale of the filamentary structure (Cargill 1993; Klimchuk & Cargill 2001). Although measurements of absolute densities in the solar corona are possible (see Ugarte-Urra et al. 2005), they are scarce.

In contrast, when studying stellar coronae, it is not possible to determine the emitting volume (other than using very general constraints based on, for example, the stellar radius, coronal scale height, and analogies with the Sun). However, broad temperature coverage can reveal features in the EM– T distribution unknown at the Sun, and a range of density-sensitive lines can provide good density diagnostics. For example, *Extreme Ultraviolet Explorer* (EUVE) observations were used by Dupree et al. (1993) to determine densities between 10^{12} and 10^{13} cm⁻³ at a temperature of 10^7 K from a small-scale source in the corona of α Aur (Capella), while in a study of the contact binary 44i Boo Brickhouse & Dupree (1998) noted that there was a dominant component of the emission measure that peaked around 10^7 K and was associated with densities of order 10^{13} cm⁻³, far higher than anything ever

measured in the solar corona. The EM of $10^{51.3}$ cm⁻³ implied a source region with scale $0.004R_*$, or a few thousand kilometers, and the sources were long-lived (i.e., not related to large flares). Sanz-Forcada et al. (2001) presented results from quiescent and flaring corona of λ And and noted that the EM peak was present in both instances. A review of these early observations and their interpretation can be found in Dupree (2002).

A more extensive survey of the EM– T distribution from active binary stars such as RS CVn and BY Dra systems, as well as single stars such as AB Dor, by Sanz-Forcada et al. (2003, hereafter SF03) revealed similar EM and density properties. SF03 showed complex EM– T distributions that they attributed to (1) solar-like loops with a modest temperature and density ($10^{6.3}$ K and $10^9\text{--}10^{10.5}$ cm⁻³, respectively), (2) hot loops similar to those discussed by Brickhouse & Dupree (1998) with $T \sim 10^{6.9}$ K and $n > 10^{12}$ cm⁻³, and (3) a very high temperature component. The second component typically has $EM > 10^{50}$ cm⁻³, and the EM– T profiles show a significant amount of plasma lying above the peak temperature. An example of such an EM– T distribution is shown in Figure 1.

In this paper we address the second of these emission sources: the sharp peak near 10^7 K. It is natural to try and understand such distributions in terms of models and data of the better studied solar corona, but this has not been successful in the past because of the difficulty in accounting for the high densities (Dupree 2002), and the component of the EM– T distribution above the peak. Conventional steady state coronal loop models (e.g., descendants of those originally developed by Rosner et al. [1978], Craig et al. [1978], Hood & Priest [1979], and Serio et al. [1981]) do not lead naturally to this form of EM– T distribution and, for typical solar coronal loop lengths, give densities 2 or 3 orders of magnitude too small (Dupree, 2002).

However, as suggested by Dupree (2002) and discussed further in § 2, another class of solar coronal heating models, namely those associated with impulsive heating (often referred to as “nanoflare” heating on account of the original assumption that the heating events had energies of 10^{24} ergs) can readily account for the observed EM– T profiles. In § 3 we adapt these models for a situation in which there is no assumed information on the size of the emitting structures and deduce the coronal parameters that correspond to the observed stellar emission. Section 4 presents a discussion of the results and, in particular,

¹ Space and Atmospheric Physics, Blackett Laboratory, Imperial College, London SW7 2BW, UK.

² Space Science Division, Naval Research Laboratory, Washington, DC 20375.

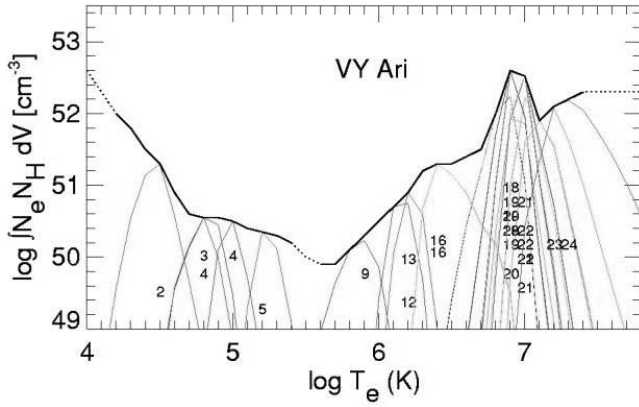


FIG. 1.—Sample EM- T distribution from VY Ari (from SF03). Note the strong peak at $T = 10^7$ K. [See the electronic edition of the *Journal* for a color version of this figure.]

addresses the implications for the magnetic field of the stellar corona.

2. IMPLICATIONS FROM THE SOLAR CORONA

In § 3 we adapt the nanoflare cooling model for the solar corona developed by Cargill (1993, 1994), Cargill & Klimchuk (1997, 2004), and Klimchuk & Cargill (2001) to address the strong peak in the EM- T distribution seen in stellar coronae. Here we discuss why this model is well suited for addressing the observed EM- T profiles. For the solar case, it is assumed that the corona is comprised of many narrow thermally isolated threads that are heated randomly by small events with energies in the range 10^{23} – 10^{25} ergs (hence the term nanoflares). A collection of many of these threads comprise the observed loop structures (see also Warren et al. 2002). The heating is assumed to be impulsive, so that the principal observed signature comes from *cooling* plasma. The cooling process is described by an energy equation of the form

$$\frac{\partial p}{\partial t} + v \frac{\partial p}{\partial s} = -\gamma p \frac{\partial v}{\partial s} + (\gamma - 1) \left[\frac{\partial}{\partial s} \left(\kappa_0 T^{5/2} \frac{\partial T}{\partial s} \right) - n^2 f(T) \right] \quad (1)$$

in the usual notation, where $\kappa_0 = 10^{-6}$ in cgs units is the thermal conductivity coefficient and $f(T)$ is the optically thin radiative loss function. If $f(T) = \chi T^\alpha$, a loop of half-length L will cool by conduction and radiation with characteristic times τ_c and τ_r , respectively, (Cargill et al. 1995, hereafter CMA95) and a ratio τ_c/τ_r :

$$\tau_c = \frac{3nkL^2}{\kappa_0 T^{5/2}}, \quad \tau_r = \frac{3kT^{1-\alpha}}{\chi n}, \quad \frac{\tau_c}{\tau_r} = \frac{\chi n^2 L^2}{\kappa_0 T^{7/2-\alpha}}. \quad (2)$$

A typical value for α is $-\frac{1}{2}$ (Priest 1982; Griffiths 1999), so conductive cooling dominates for hot, tenuous loops, and radiative cooling for cool, dense loops, with the ratio of cooling times as defined in equation (2) increasing from small to large as a loop cools. Both cooling mechanisms have associated mass motions: the conductive phase is believed to drive an upflow from the chromosphere into the loop (Antiochos & Sturrock 1978), while the radiative phase is associated with a downflow toward the chromosphere (Antiochos 1980; CMA95, Bradshaw & Cargill 2005). Thus, the loop density takes on its maximum value when the cooling changes from conduction to radiation (see also Warren et al. 2002). This is also when the instantaneous cooling time is maximized.

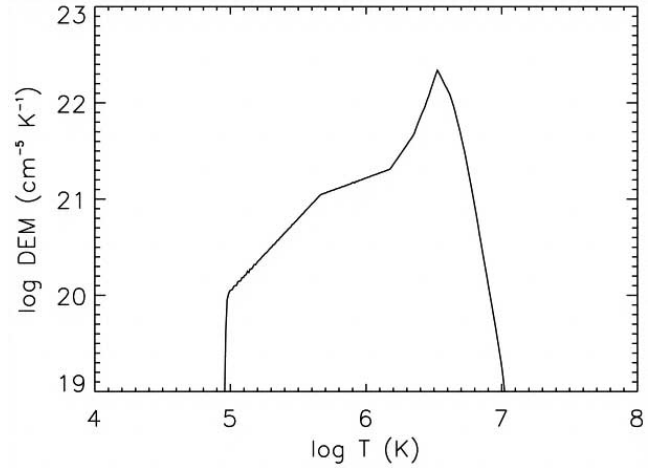


FIG. 2.—Differential emission measure from a nanoflare model of the solar corona (from Klimchuk & Cargill 2001).

To understand the implications of this for stellar EM- T distributions, we show a case discussed previously in Cargill & Klimchuk (1997, 2004) and Klimchuk & Cargill (2001) of an active region loop heated by many millions of nanoflares. The details can be found in these papers, but in Figure 2 we show an EM- T distribution. A strong peak around $10^{6.5}$ K is clearly evident: to the right of this temperature, loops cool by conduction and to the left by radiation. There are thus significant amounts of plasma on both sides of the peak, as seen in the stellar observations. The task now is to adapt this model from a situation in which the input parameters include the loop length, to one in which it is unknown.

3. APPLICATION TO STELLAR CORONAE

3.1. Analytic Description of Multistrand Coronal Model

Later in this section we present some numerical results for stellar coronae, but we first make use of the analytic approach developed by Cargill (1993, 1994) and Cargill & Klimchuk (2004). In these papers, we showed that for given loop dimensions, simple scalings relate the temperature and emission measure at the peak of the EM- T distribution to the nanoflare energy. We must now adapt this to stellar coronae, while retaining the following assumptions: (1) the emission comes from an ensemble of loop-like structures (or strands) of typical length $2L$, with the plasma confined by the magnetic field; (2) these strands are heated by a swarm of small impulsive heating events, but there is no a priori assumption made about the energy in the events, although for convenience, we retain the word “nanoflare”; (3) the heated strands cool by the two-part process described in § 2; and (4) the strands cool completely to subcoronal temperatures before they are reheated. The final assumption is relaxed in our numerical results in § 3.2.

The temperature where the EM- T distribution peaks (hereafter the peak temperature) arises approximately when $\tau_c = \tau_r$, so that we can relate the peak temperature, density, and loop length to each other. We assume that the density corresponding to the peak of the EM- T distribution (hereafter the peak density) can be determined approximately from the ratios of appropriate density-sensitive pairs of iron lines (SF03). For simplicity we define the radiative loss function as $f(T) = \chi T^{-1/2}$ with $\chi = 8 \times 10^{-20}$. (This is a slight modification of the form proposed by Griffiths [1999], who suggested that it is valid in the range $10^{6.8}$ K $< T < 10^{7.4}$ K. However, it seems likely that a

bremsstrahlung component proportional to $T^{1/2}$ will become important at the upper end of this temperature range.) For a measured peak temperature and density, the loop half-length is determined from equation (2) by

$$L = \frac{T^2}{n} \sqrt{\frac{\kappa_0}{\chi}} = 3.54 \times 10^8 \left(\frac{T}{10^7}\right)^2 \left(\frac{10^{12}}{n}\right) \text{ cm} \quad (3)$$

(Note that the values of L determined from eq. [3] are uncertain by a factor of at least 2 on the short side due to the approximate way the conductive losses are treated. Specifically, the approximate model using eq. [2] neglects numerical factors that arise in a more precise solution of the heat conduction equation [e.g., Antiochos & Sturrock 1978].) The conductive and radiative cooling times at the EM- T peak are then $\tau_c = \tau_r = 163(T/10^7)^{3/2}(10^{12}/n)$ s.

The lack of imaging means that we cannot make any precise statements about the scale of any coronal structures, although Brickhouse & Dupree (1998) inferred this from density and emission measure measurements. Instead we assume that the strands each have a diameter Δl and that N such strands are available to produce the entire coronal emission. Therefore, the total volume from which emission is feasible is $2L\pi(\Delta l/2)^2N$, although not all the strands need be filled with plasma at any time. For sudden heating by a nanoflare of energy Q , the postheating plasma parameters in a strand satisfy $6nkTL\pi(\Delta l/2)^2 = Q$. Because the pressure remains approximately constant during the conductive cooling phase, this relationship is also valid at the time of the peak of the EM- T distribution. Using equation (3) one finds

$$\begin{aligned} \Delta l &= 2\sqrt{\frac{Q}{6nkTL\pi}} = 2\left(\frac{\chi}{\kappa_0}\right)^{1/4} \sqrt{\frac{Q}{6\pi k T^3}} \\ &= 6.6 \times 10^5 \sqrt{\left(\frac{Q}{10^{24}}\right) \left(\frac{10^7}{T}\right)^3} \text{ cm}. \end{aligned} \quad (4)$$

The solar EM- T distributions discussed in § 2 are often representative of loops having what are said to be small “filling factors.” The definition of a filling factor in the solar corona is the ratio of the volume of plasma that actually contains radiating material to the total volume of the loop system. The determination of the solar filling factor requires the calculation of the density from line pairs, and an “average” density from the emission measure, which in turn requires an estimate of the volume. The filling factor is thus both a measure of how poorly imaging instruments resolve the actual coronal structure and of the scale of the coronal energy release (Cargill 1994; Cargill & Klimchuk 1997).

However, in the absence of images, a filling factor based on such a definition has no meaning. Instead, we define the stellar filling factor to be the ratio of the number of strands filled with radiating plasma to N . Note that the following analysis is only valid for a small filling factor, since we require the strand to cool below coronal temperatures before being reheated (Cargill, 1993). Indeed, when a strand is reheated frequently, its temperature and density remain around one pair of values, and one approaches a steady state model that gives a different EM- T profile from that seen. Cooling strands produce a broad EM- T distribution.

We follow Cargill (1993, 1994) and Cargill & Klimchuk (2004) and define the filling factor as $\phi = \tau_{\text{cool}}/\tau_{\text{nano}}$, where τ_{cool} is the loop cooling time (defined in our earlier papers) and $\tau_{\text{nano}} = NQ/E_T$ is the characteristic interval between nanoflares in a given strand, with E_T being the total coronal energy requirements in

ergs per second. Following the approach of Cargill & Klimchuk (2004), we find

$$\begin{aligned} \phi &= \frac{5kLE_T\Delta l^{1/3}}{NQ^{7/6}} \left[\frac{(3k\pi)^2}{4\kappa_0^5\chi^7}\right]^{1/12} \\ &= \frac{5kE_T T^{3/2}}{NQ\chi n} = \frac{273}{N} \left(\frac{E_T}{Q}\right) \left(\frac{10^{12}}{n}\right) \left(\frac{T}{10^7}\right)^{3/2}. \end{aligned} \quad (5)$$

Defining the emission measure at the peak of the distribution as $\text{EM}^* = n^2 V_R$, where $V_R = N\phi 2L\pi(\Delta l/2)^2$ is the total emitting volume, and using equations (3), (4), and (5) to substitute for L , Δl , and ϕ , respectively, we find

$$\begin{aligned} \text{EM}^* &= N\phi n^2 2L\pi \left(\frac{\Delta l}{2}\right)^2 = \frac{5}{3} \frac{E_T}{\chi T^{-1/2}} \\ &= 6.6 \times 10^{46} \left(\frac{E_T}{10^{24}}\right) \left(\frac{T}{10^7}\right)^{1/2}. \end{aligned} \quad (6)$$

One can then eliminate E_T from equations (5) and (6) to derive an expression for the filling factor in terms of the observed independent quantities T , EM, and n :

$$\phi = \frac{3kT\text{EM}^*}{nQN} = \frac{4.1 \times 10^5}{N} \left(\frac{10^{24}}{Q}\right) \left(\frac{\text{EM}^*}{10^{50}}\right) \left(\frac{10^{12}}{n}\right) \left(\frac{T}{10^7}\right). \quad (7)$$

The actual coronal volume radiating at any given time is

$$V_R = 10^{26} \left(\frac{\text{EM}^*}{10^{50}}\right) \left(\frac{10^{12}}{n}\right)^2 \text{ cm}^3 = 2.9 \times 10^{-7} \left(\frac{\text{EM}^*}{10^{50}}\right) \left(\frac{10^{12}}{n}\right)^2 R_s^3, \quad (8)$$

which gives scales (l_R) of around $l_R \sim 10^{-2}R_s$, similar to those noted by Brickhouse & Dupree (1998). However, the total coronal volume that participates in the emission over a long time depends on ϕ and is given by $V_T = V_R/\phi$; this can be of order $0.1R_s$ for small filling factors.

A *maximum* nanoflare energy permitted in this model (Q_{max}) can be derived from equation (4) by assuming $\Delta l < L$:

$$Q_{\text{max}} = \frac{3\pi k}{2} \left(\frac{\kappa_0}{\chi}\right)^{3/2} \frac{T^7}{n^2} = 2.87 \times 10^{29} \left(\frac{T}{10^7}\right)^7 \left(\frac{10^{12}}{n}\right)^2 \text{ ergs}. \quad (9)$$

If $\Delta l \ll L$, then Q_{max} will be smaller. This gives a *minimum* filling factor (ϕ_{min}) of

$$\phi_{\text{min}} = \frac{2n\text{EM}^*}{\pi NT^6} \left(\frac{\chi}{\kappa_0}\right)^{3/2} = \frac{1.44}{N} \left(\frac{n}{10^{12}}\right) \left(\frac{\text{EM}^*}{10^{50}}\right) \left(\frac{10^7}{T}\right)^6. \quad (10)$$

We have summarized the results presented by SF03 in Table 1. Of the 21 stars in the SF03 list, four are neglected. Three are classed as “low activity stars” by SF03 (ϵ Eri, Procyon, and α Cen) and do not show the characteristic EM- T peak at high temperatures. Procyon and α Cen have the EM- T peak at $10^{6.3}$ – $10^{6.4}$ K, and while ϵ Eri has emission up to $10^{6.9}$ K, the distribution is flat rather than peaked. LQ Hya is omitted because of the absence of electron density measurements in SF03. All quantities are shown as logarithms. The parameter N is chosen as 10^6 . This

TABLE 1
RESULTS

Star (1)	EM* (cm ⁻³) (2)	T (K) (3)	n (cm ⁻³) (4)	l _T (R _⊙) (5)	L (cm) (6)	Q _{max} (ergs) (7)	ϕ _{min} (8)	B (G) (9)
AY Cet (G5/WD).....	52.7	6.9	12.7	-1.13	7.65	27.36	-1.84	2.72
AR Psc (G7/K1).....	51.8	7.0	13.1	-1.33	7.45	27.26	-2.94	2.97
CC Eri (K7/M3).....	51.2	6.9	13.3	-1.73	7.05	26.16	-2.74	3.02
VY Ari (K3).....	52.6	6.9	13.4	-1.83	6.95	25.96	-1.24	3.07
YY Gem (M1/M1).....	51.2	6.9	13.2	-1.63	7.15	26.36	-2.84	2.97
BF Lyn (K2).....	51.6	6.7	12.9	-1.73	7.05	25.56	-1.54	2.72
DH Leo (K0/K7).....	51.9	6.8	12.4	-1.03	7.75	27.26	-2.34	2.52
ξ UMa (G5/K).....	51.1	6.8	12.0	-0.63	8.15	28.06	-3.54	2.32
BH Cvn (F2/K2).....	52.1	6.9	13.1	-1.53	7.25	26.56	-2.04	2.92
s2 CrB (F6/G0).....	52.3	6.7	13.0	-1.83	6.95	25.36	-0.74	2.77
V824 Ara (G5/K0).....	52.4	6.9	12.3	-0.73	8.05	28.16	-2.54	2.52
V478 Lyr (G8).....	51.9	6.8	12.7	-1.33	7.45	26.66	-2.04	2.67
ER Vul (G0/G5).....	52.3	6.8	12.4	-1.03	7.75	27.26	-1.94	2.52
AR Lac (G2/K0).....	52.4	6.9	12.8	-1.23	7.55	27.16	-2.04	2.77
AR Lac 2 (G2/K0).....	52.5	6.9	13.2	-1.63	7.15	26.36	-1.54	2.97
Fk Aqr (M2/M3).....	50.9	6.9	12.6	-1.03	7.75	27.56	-3.74	2.67
BY Dra (K4/K7).....	51.6	6.8	13.3	-1.93	6.85	25.46	-1.74	2.97

NOTES.— Columns (1)–(6) show the star(s) and spectral type(s) taken from SF03, the emission measure, temperature, and density at the peak of the EM-*T* distribution, the characteristic scale of the emission, and the half-length calculated from eq. (3), respectively. Columns (7) and (8) show, respectively, the maximum heating event energy and the minimum filling factor (eqs. [9] and [10]) for a corona with $N = 10^6$. Column (9) shows the magnetic field intensity needed to confine the plasma. All numbers are on a log scale.

is motivated by the desire to have values of $\phi_{\min} \ll 1$ and to have the characteristic overall coronal scale $l_T \sim V_T^{-1/3}$ a small fraction of a radius. Values of order 10^6 meet these requirements: smaller (larger) values of N give large filling factors (large volumes) for some cases.

Columns (1)–(4) show the star and its spectral type (using the notation of SF03), the peak emission measure, the temperature at that peak, and the estimated density. Some comments are necessary. The peak emission measure and temperature were determined from Table 8 of SFD03. The density is taken as being the mean of measurements using a number of iron line ratios (SF03, Table 6). The errors quoted in the density measurements are typically between 0.2 and 0.6 on a log scale. Note also that the time to establish ionization equilibrium is very short because of the high densities and is much shorter than the cooling time.

Columns (5) and (6) show the characteristic scale of the emission (l_T as defined above) in units of a solar radius, and the values of L calculated from equation (3), respectively. We have calculated l_T from the emission measure, density, and minimum filling factor, and note that the values range around $10^{-2} R_{\odot}$. Columns (7) and (8) of the table show, respectively, the maximum nanoflare energy and the minimum filling factor when $N = 10^6$, as calculated from equations (9) and (10). Column (9) shows the magnetic field intensity in gauss needed to confine a plasma with the peak density and temperature. We discuss these in turn:

1. The typical calculated loop size ($2L$) lies between roughly 200 and 2000 km, although we stress that the treatment of conduction implies this is underestimated. These values of L are those required in an impulsive heating model to give the peak in the emission measure curve at the measured temperature. They are, of course, much smaller than the “characteristic” length scales (l_R and l_T), because the total emitting volume comprises many loops of dimension $2L$. They are also much smaller than typical loops in the solar corona.

2. The maximum energies mostly lie in the range 10^{26} – 10^{28} ergs, bigger than those believed to occur in the quiescent

solar corona, but of order observed solar microflares. It is not surprising that the energies are larger than their quiescent solar counterparts, since the energy is likely to scale with B^2 , and the magnetic field in these stellar loops is much stronger as we discuss in a moment.

3. The minimum filling factors are all small, in many cases $\ll 1$, hence consistent with the assumptions of our model.

4. The magnetic field required to confine the plasma is between a few hundred gauss and 1 kG. This should not be confused with the coronal magnetic field, which will almost certainly be larger.

The scalings with Q and N are obvious. For a fixed N , when Q is smaller than the maximum value, the filling factor increases. As N increases (decreases), the filling factors decrease (increase).

3.2. Numerical Results

The above analytical model, while shedding light on the origin of the EM-*T* peaks, is limited in many ways. It can only accommodate a single power-law radiative loss function, can only model energy release with one value of Q , and assumes the loop cools completely before reheating. However, this approach can be readily adapted to a numerical model that eliminates these constraints. Cargill (1994) introduced such a model (see also Cargill & Klimchuk 1997, 2004; Klimchuk & Cargill 2001) in which the heating and cooling of many thousand strands can be modeled. We demonstrate this approach for the corona of AR Lac with a peak emission measure of $10^{52.4} \text{ cm}^{-3}$ and a peak temperature and density of $10^{6.9} \text{ K}$ and $10^{12.8} \text{ cm}^{-3}$, respectively. The six-part radiative loss function presented in Klimchuk & Cargill (2001) is used. The multistrand model has been run for the analytic example in § 3.1 and gives good agreement between the input and output.

The approach is as follows. The loop length is determined from the peak density and temperature using equation (3) (354 km in this case). The total energy required per second comes from equation (6), modified slightly to account for the more accurate

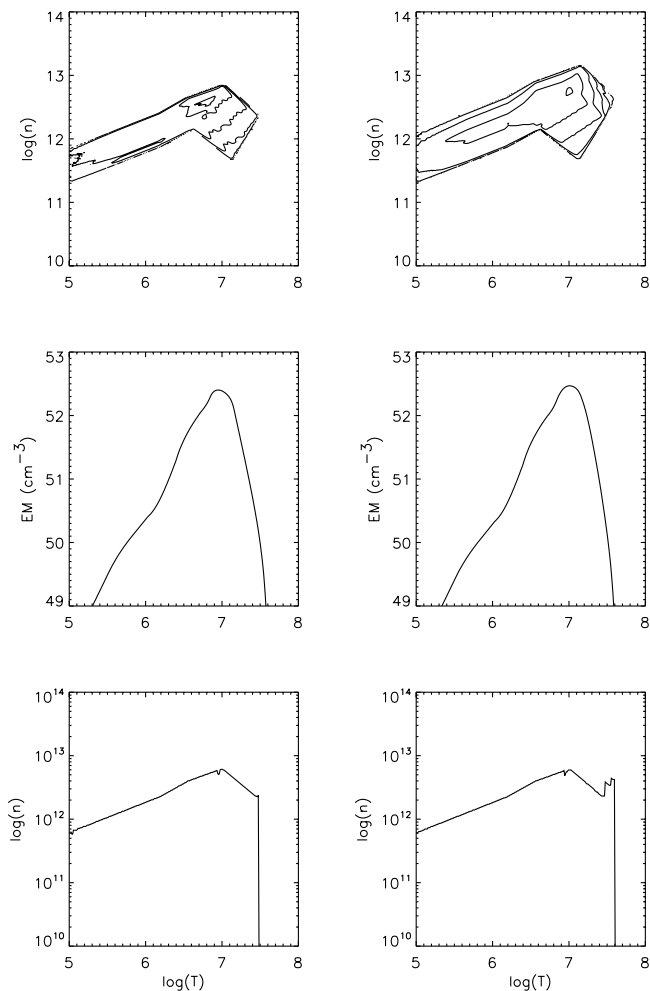


FIG. 3.—*Left*: Emission measure differential in density and temperature, where the emission measure is integrated over density and a temperature interval of $\log(\Delta T)$, and the maximum density as a function of temperature for a case in which $\Delta l = L$ for the corona of AR Lac. The heating events are randomly distributed in the range $2 \times 10^{26} - 2 \times 10^{27}$ ergs. The right column has the same parameters except $\Delta l = L/5$.

loss function. A range of nanoflare energies subject to condition (9) is used, as described below. One can generate a range of models by looking at different values of Δl , Q , and N . For all examples we assume $N = 10^6$.

Figure 3 shows results in a similar (but compressed) format to that in Cargill & Klimchuk (2004). The two columns are for a collection of loops with a total energy loss of 7×10^{29} ergs s^{-1} , but the left (*right*) panels have $\Delta l = L$ and a nanoflare energy range randomly distributed between $2 \times 10^{26} - 2 \times 10^{27}$ ergs ($\Delta l = L/5$ and a nanoflare range between 8×10^{24} and 8×10^{25} ergs). From top to bottom, we show a contour plot of the emission measure differential in temperature and density, the emission measure from all strands as a function of temperature integrated over a temperature range $T \pm \Delta \log T$, with $\Delta \log T = 0.15$, and the maximum density (not to be confused with the “peak” density defined previously as the density of peak EM) as a function of temperature. The filling factor in each case is 0.014 and 0.28, respectively.

The figure shows the following:

1. The emission measure differential in temperature and density is a measure of the distribution of density and temperature in the strands. It is clear that the emission comes from a wide range of temperatures and densities, with the highest density

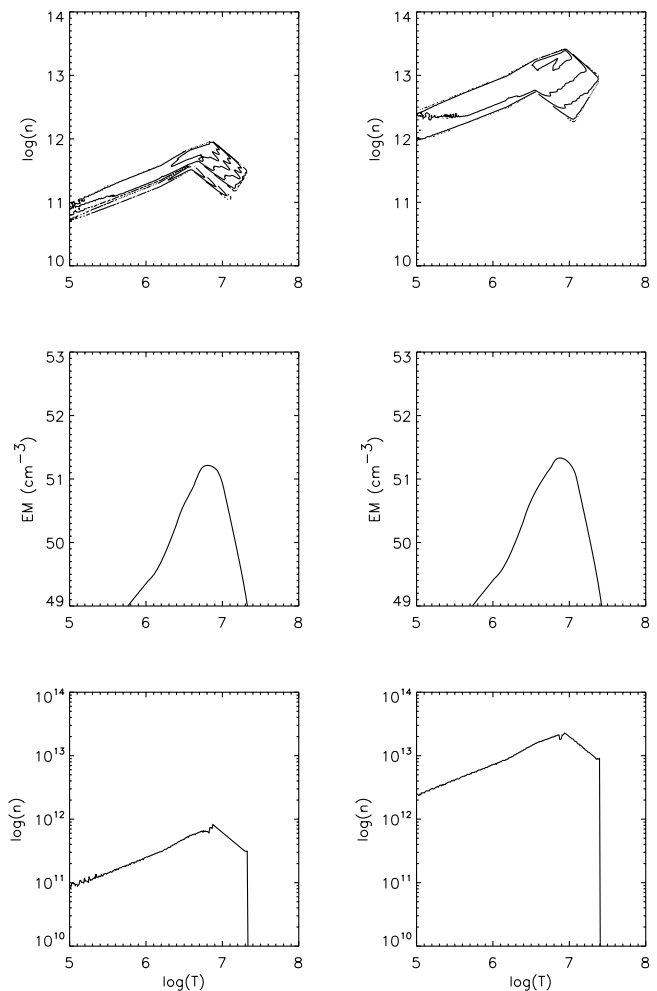


FIG. 4.—Same as Fig. 3, but for ξ UMa (*left*) and BY Dra (*right*).

plasma generally being associated with the highest temperature. However, these results also show the existence of plasma over all temperature ranges from a few times 10^7 to 10^5 K, as seen in the observed emission measures. For a given temperature, plasma exists over a range $\Delta \log n = \pm 0.5$, and for a given density, the temperature range is $\Delta \log T = \pm 0.4$ or so. Decreasing Δl for a fixed range of Q leads to a broader range of densities, especially at the high-density end (see eq. [4]).

2. For both cases, the total emission measure peaks near $10^{52.4}$ cm^{-3} at a temperature of 10^7 K and shows a steep falloff with temperature on *either* side of the peak. The slope (defined as $d \log EM / d \log T$) is over 2, taking on a value of 2.3.

3. The density distribution peaks somewhat below 10^{13} cm^{-3} at a temperature of 10^7 K. Thus, the overall properties of the emission measure, density, and temperature are reproduced in the model.

4. The filling factor is small.

Figure 4 shows results from two other stars: ξ UMa (*left*) and BY Dra (*right*) that have significantly lower and higher densities than AR Lac. The parameters in each case are $L = 1.4 \times 10^8$ and 7.1×10^6 cm, and the range of energies is between 10^{27} and 10^{28} ergs and 3×10^{24} to 3×10^{25} ergs, respectively. We see that the model again is able to give the general shape of the EM- T curves.

4. DISCUSSION

We have presented a simple model to account for the strong peaks in the emission from active binary coronae at around 10^7 K.

Such emission measure distributions are very reminiscent of those predicted in a solar corona heated by impulsive events. The coronal scenario can be readily adapted to the stellar case with the relevant emission measures and densities being produced by a number of short magnetic loops occupying a small fraction of the stellar surface.

It is natural to relate these results to the solar corona. The loop sizes are reminiscent of X-ray bright points, the event energies are typical of microflares, the temperatures are characteristic of solar flares, and the densities are larger than anything ever measured at the Sun. As has been shown by Testa et al. (2005), classical loop models can give high temperatures and emission measures for loops with lengths of order 10^{10} cm, but the densities in such a model are too small by up to 3 orders of magnitude.

How are we to understand the major source of emission coming from very small loop sizes (as also predicted by Brickhouse & Dupree [1998]) in the context of what we know about the magnetic activity of the Sun and stars? One can immediately calculate the magnetic field having an energy density equivalent to that of the hot plasma: this is given in column (9) of Table 1 and is typically at least a few hundred gauss. The field must be stronger than this in order to confine the plasma. If one then recalls that coronal reconnection needs a nonpotential field and that perhaps this component is 25% of the total, one then has field strength well in excess of 1 kG.

It seems that a requirement is the continual presence of many small magnetic structures that brighten, flicker, and die over a short time. These structures may extend over a significant part of the surface of a star. This would imply that the emission from such stars is dominated not by active regions as at the Sun, but by regions of very mixed magnetic polarity. Whether this is

similar to the magnetic carpet on the Sun, but operating more effectively, remains to be determined. We can speculate that a surface dynamo, which produces mixed polarities, is stronger in these stars than a deep-seated tachocline-type dynamo, which produces active regions (although see Schrijver 2005).

In this paper we have argued that a process similar to solar nanoflares operates implying that the coronal field is stressed by continual footpoint motions. One can use Poynting's theorem to show that the velocities required for this are

$$v = \frac{2Q}{B_t B_l (\Delta l / 2)^2 \tau_{\text{nano}}},$$

where B_t and B_l are the field components along the loop axis and in the transverse direction respectively. Simulations suggest a ratio B_t/B_l between 0.25 and 0.5 (e.g., Dahlburg et al. 2005). Taking $Q = 10^{27}$ ergs, $B_l = 1$ kG, $\Delta l = 100$ km, and $\tau_{\text{nano}} = 1000$ s, we find $v = 3.2$ km s $^{-1}$, a reasonable number. The scalings with the parameters are obvious. Alternatively, one might have a heating scenario in which small-scale flux elements emerge and immediately reconnect with an overlying field, hence giving an impulsively heated, confined plasma. However, this may give a pair of loops, one short and one long, that would not be consistent with the EM-T profile.

P. C. acknowledges the support of a PPARC Senior Research Fellowship. J. A. K. thanks ONR and NASA for support. We thank Andrea Dupree for encouraging us to carry out this investigation and for providing Figure 1.

REFERENCES

- Antiochos, S. K. 1980, *ApJ*, 241, 385
 Antiochos, S. K., & Sturrock, P. A. 1978, *ApJ*, 220, 1137
 Bradshaw, S. J., & Cargill, P. J. 2005, *A&A*, 437, 311
 Brickhouse, N. S., & Dupree, A. K. 1998, *ApJ*, 502, 918
 Cargill, P. J. 1993, *Sol. Phys.*, 147, 263
 ———. 1994, *ApJ*, 422, 381
 Cargill, P. J., & Klimchuk, J. A. 1997, *ApJ*, 478, 799
 ———. 2004, *ApJ*, 605, 911
 Cargill, P. J., Mariska, J. T., & Antiochos, S. K. 1995, *ApJ*, 439, 1034 (CMA95)
 Craig, I. J. D., McClymont, A. N., & Underwood, J. H. 1978, *A&A*, 70, 1
 Dahlburg, R. B., Klimchuk, J. A., & Antiochos, S. K. 2005, *ApJ*, 622, 1191
 Dupree, A. K. 2002, in *ASP Conf. Ser. 277, Stellar Coronae in the Chandra and XMM-Newton Era*, ed. F. Favata and, J. J. Drake (San Francisco: ASP), 201
 Dupree, A. K., Brickhouse, N. S., Doschek, G. A., Green, J. C., & Raymond, J. C. 1993, *ApJ*, 418, L41
 Griffiths, N. W. 1999, *ApJ*, 518, 873
 Hood, A. W., & Priest, E. R. 1979, *A&A*, 77, 233
 Klimchuk, J. A., & Cargill, P. J. 2001, *ApJ*, 553, 440
 Priest, E. R. 1982, *Solar Magnetohydrodynamics* (Dordrecht: Reidel)
 Rosner, R., Tucker, W. H., & Vaiana, G. S. 1978, *ApJ*, 220, 643
 Sanz-Forcada, J., Brickhouse, N. S., & Dupree, A. K. 2001, *ApJ*, 554, 1079
 ———. 2003, *ApJS*, 145, 147 (SF03)
 Schrijver, C. J. 2005, in *Proceedings of the International Scientific Conference on Chromospheric and Coronal Magnetic Fields*, ed. S. Solanki (ESA SP-596; Noordwijk: ESA), 32
 Serio, S., et al. 1981, *ApJ*, 243, 288
 Testa, P., Peres, G., & Reale, F. 2005, *ApJ*, 622, 695
 Ugarte-Urra, I., Doyle, J. G., Walsh, R. W., & Madjarska, M. S. 2005, *A&A*, 439, 351
 Warren, H., Winebarger, A., & Mariska, J. T. 2002, *ApJ*, 579, L41